Vibrational spectra of cyclic C_8 in solid argon[1]

José Domingo Presilla-Márquez [2], Jessica Harper, Jeffrey A. Sheehy,
Patrick G. Carrick, and C. William Larson

*Propulsion Sciences and Advanced Concepts Division, AFRL/PRS, Air Force Research Laboratory,
10 E. Saturn Blvd., Edwards AFB, California 93524-7680 USA*

Submitted 22 October 1997
Revised 20 October 1998

Abstract

Vapors from solid and powdered carbon, emitted from an oven cycled between 2000 and 3000 K, were co-condensed with argon onto a CsI substrate maintained at 10 K. The cycling process produced a multilayered matrix with regions of high carbon density alternating with layers of argon. FTIR measurements including complete ^{13}C isotopic data, supported by *ab initio* calculations, allow the assignment of a band observed at 1817.8 cm^{-1} to the $\nu_{12}(e_u)$ fundamental of cyclic C_8, correcting an erroneous assignment of this band in the recent literature.

---

[1] Presented in part at the 52nd Ohio State University International Symposium on Molecular Spectroscopy, Columbus, OH, June 16-20, 1997.

[2] Present address: Schafer Corporation, 26565 W. Agoura Road, Suite 202, Calabasas, CA 91302

1. Introduction

The US Air Force High Energy Density Matter (HEDM) Program is examining the feasibility of using cryogenic solids seeded with energetic species as rocket propellants [1]. In the course of this work, attempts to deposit carbon atoms in solid argon resulted in the first conclusive identification of cyclic C_6 [2], which appeared as the most abundant condensation product. This observation suggested that other small cyclic neutral polycarbons also may have been present, as quantum-chemical calculations predict that each of the C_{2n} (n = 2-9) clusters have cyclic isomers that are more stable than their linear counterparts [3-6].

There have been several computational studies of the structures, energetics, and infrared spectra of C_8 isomers [3-6]. The extensive electron-correlation calculations of Martin and Taylor [6], employing single- and double-excitation coupled-cluster wave functions with a noniterative treatment of connected triple excitations [CCSD(T)], predict that a cyclic polyacetylenic isomer (C_{4h} symmetry, ^1A_g electronic state) is 8 ± 2 kcal/mol lower in energy than the linear chain ($D_{\infty h}$, $^3\Sigma_g^-$). This ordering of isomer energies agrees with earlier predictions by Raghavachari and Binkley [3].

Linear C_8 was first identified by Van Zee *et al.* [7] in electron-spin-resonance studies of laser-vaporized graphite trapped in solid neon. Szczepanski *et al.* [8] subsequently used theoretical results to interpret their own infrared spectroscopic measurements of carbon clusters trapped in argon matrices, concluding that absorptions at 2071.5 and 1710.5 cm^{-1} could originate from linear C_8. In our recent letter on cyclic C_6 [2], we confirmed the assignment of the 1710.5 cm^{-1} band to the $\nu_9(\sigma_u)$ mode of linear C_8, which is consistent with recent measurements of linear C_8 vibrational frequencies in neon matrices [9]. Additionally, we measured a constant intensity ratio of 2.7:1 between the two bands throughout several experiments, in accord with the

2

observation of Szczepanski et al. [8]. Electronic transitions of linear C_8 and C_8^- have also been studied [10-12].

By contrast, experimental evidence for **cyclic** C_8 is scarce. Based on *ab initio* calculations, Martin and Taylor [6] suggested that an absorption at 1818 cm^{-1}, first observed but unassigned by Thompson et al. [13], could belong to this species. Recently, however, Wang et al. [14] assigned the $\nu_{12}(e_u)$ fundamental of cyclic C_8 to a band at 1844.2 cm^{-1}, which was observed in the spectra of matrices produced by trapping laser-ablated carbon in solid argon. In the present work, we confirm the former and refute the latter claim by conclusively assigning a band at 1817.8 cm^{-1} to the $\nu_{12}(e_u)$ fundamental of cyclic C_8, which was observed as the second most abundant condensation product in the same argon matrices that contained cyclic C_6 [2].

2. Computational methods

Although calculated harmonic frequencies and, in some cases, infrared intensities for unsubstituted cyclic C_8 have been reported [3-6], the spectral shifts of $^{13}C_n{}^{12}C_{8-n}$ ($n = 1$-8) isotopomers relative to $^{12}C_8$ are generally not available. To obtain these values, which are essential for definitive identification of matrix-isolated species, we performed density-functional (B3LYP) calculations [15] in cc-pVDZ [16], cc-pVTZ [16], and 6-311G($2d$) [17] atomic basis sets, as well as CCSD(T) calculations [18] in the cc-pVDZ basis. The Gaussian 94 [17] program system was used on IBM RS/6000 work stations at the Air Force Research Laboratory and a Cray C90 computer at the Department of Defense Aeronautical Systems Center.

3. Experimental methods

Mixtures of carbon-12 and carbon-13 powders (~ 100 mg total), in varying ratios, were resistively heated in a tantalum oven lined with an approximately equal mass of solid graphite. The vapors escaping through a small orifice were co-deposited with continuously flowing argon onto a CsI substrate maintained at 10 K. The procedures followed in the initial heating of the oven were similar to those used in our matrix study of BC_2 [19], whereas other aspects of the experiment are described elsewhere [2]. Here we focus on the method of cycling the oven temperature during the course of a deposition, which produced a matrix with alternating layers of high carbon density and nearly pure argon.

Once the oven temperature reached 2900 K, the first cycle began with the opening of a gate valve separating the furnace from the substrate. The oven temperature was held constant for 3 min while a carbon-rich layer of approximately 3 μm thickness was deposited. The applied power was then quickly decreased to a level that yielded a steady-state temperature of about 2000 K. After a 1 min pause, the temperature (power) was manually increased by 300 K/min to 2900-3000 K; this heating rate was chosen specifically to minimize particle ejection. This completed the first of ten cycles; there was no time lapse between successive cycles.

Cyclic C_8 was detected in the same three matrices, labeled (a), (b), and (c) in Fig. 1, that contained cyclic C_6 [2]. The average ^{13}C isotopic enrichment of matrices (b) and (c) was approximately 25% and 50%, respectively, relative to the natural abundance matrix (a). Survey FTIR spectra of these matrices, as deposited and after several annealings, were recorded with a Mattson Cygnus 100 spectrometer at a resolution of 1 cm^{-1} using a liquid nitrogen cooled Hg-Cd-Te (MCT) detector and a KBr beamsplitter for scans in the mid-infrared region of the

spectrum (400-4000 cm^{-1}). The procedure for recording the spectra and annealing the matrices has been described previously [2,19].

4. Results and discussion

Figure 1(a)-(c) shows spectra between 1740 and 1830 cm^{-1} of matrices annealed to 27.5 K. The 1817.8 cm^{-1} absorption, the dominant feature of Fig. 1(a), is the same band seen by Krätschmer and Nachtigall [20], tentatively assigned to cyclic C_8 by Martin and Taylor [6] based on CCSD(T)/cc-pVDZ calculations. The harmonic frequencies and infrared intensities for cyclic $^{12}C_8$ that resulted from our isotopic shift calculations are listed in Table 1. These show that the computed vibrational spectrum is relatively insensitive to the choice of atomic basis set and correlation treatment; each calculation predicts an intense $\nu_{12}(e_u)$ mode, in accord with other studies [4-6]. The scale factor that brings the calculated B3LYP/cc-pVDZ frequency of this mode into coincidence with 1817.8 cm^{-1} is 0.939334, sufficiently near unity to suggest that this band is the $\nu_{12}(e_u)$ fundamental. Applying this same scale factor to calculated isotopomer frequencies gives specific assignments to the bands in Fig. 1.

The seventy distinct $^{13}C_n{}^{12}C_{8-n}$ isotopomers belong to one of three symmetry point groups: only four have the C_{4h} symmetry of unsubstituted $^{12}C_8$, whereas six are C_{2h} and sixty are C_s. For C_{2h} and C_s isotopomers the degeneracy of the ν_{12} mode is lifted, giving rise to absorptions that may be designated "ν_{12A}" and "ν_{12B}," as indicated in Table 2. Additionally, the $\nu_1(a_g)$ and $\nu_4(b_g)$ modes of the parent $^{12}C_8$ molecule become active in C_s isotopomers, and many of these bands appear with significant intensity in the same 70 cm^{-1} interval that contains the 136 bands arising from the ν_{12A} and ν_{12B} fundamentals. This creates an extremely dense spectrum, particularly between 1765 and 1790 cm^{-1}, rendering specific isotopomer assignments somewhat provisional.

5

Table 2 summarizes computed frequencies and assignments to bands in Fig. 1 for $^{12}C_8$, $^{13}C_8$, and their singly and doubly substituted isotopomers. The cyclic $^{13}C_8$ isotopomer appears at 1748.2 cm^{-1} in Fig. 1(c), exhibiting a $^{12}C_8$ to $^{13}C_8$ isotopic shift of -69.6 cm^{-1}, in good agreement with the scaled calculated shift of -71.5 cm^{-1}. Two of the four bands arising from $^{13}C_1{}^{12}C_7$ isotopomers are prominent in Fig. 1(b), but they are less evident in Fig. 1(c), where the spectrum is dominated by more highly substituted isotopomers. Their isotopic shifts of -12.7 and -15.5 cm^{-1}, respectively, compare well with the scaled calculated values of -13.2 and -15.1 cm^{-1}. As indicated in Table 2, the other two $^{13}C_1{}^{12}C_7$ isotopomer bands are within the envelope of the main 1817.8 cm^{-1} absorption. Similarly, two of the bands arising from $^{13}C_7{}^{12}C_1$ isotopomers are seen superimposed in Fig. 1(c) at 1752.2 cm^{-1}, whereas the others are coincident with the absorption at 1748.2 cm^{-1}. Once again, the isotopic shifts of -65.6 and -69.6 cm^{-1} are in good accord with the calculations (Table 2). An attempt has been made to identify the twenty-eight bands arising from the doubly substituted ($^{12}C_6{}^{13}C_2$) and doubly unsubstituted ($^{12}C_2{}^{13}C_6$) isotopomers; these assignments are indicated in Table 2, but they should not be considered definitive due to spectral congestion. Additionally, other prominent features are evident, such as the band at 1797.7 cm^{-1} [Fig. 1(b)-(c)], which results from one $^{13}C_4{}^{12}C_4$ isotopomer of the ν_{12} mode as well as two $^{13}C_4{}^{12}C_4$ and two $^{13}C_5{}^{12}C_3$ isotopomers arising from the ν_1 mode.

An additional factor that gives rise to the interesting spectral profile of Fig. 1(c), with sharper peaks near the ends and a less distinct central region, is the variation over the course of an experiment in the types of $^{13}C_n{}^{12}C_{8-n}$ isotopomers formed. Since the powders are evaporated more readily than the solid graphite liner, the carbon content of the first few layers of the matrix corresponds closely to the composition of the powders, whereas layers deposited later are richer in ^{12}C due to evaporation of the natural-abundance graphite liner. Figure 2 shows spectra

obtained from matrix (c) after each of three annealings, which produced a threefold increase in the integrated absorbance over the spectrum of the originally deposited matrix. Clearly, the features observed between 1817 cm^{-1} and 1748 cm^{-1} result from isotopomers of a single molecule, because each peak and valley is well correlated as the matrix is repeatedly annealed.

In the course of this and previous work [2], we have calculated infrared frequencies, intensities, and isotopic shifts for all linear C_n (n = 3-13) and cyclic C_{2n} (n = 2-6) clusters, following the work of Martin et $al.$ [5]. Our calculations for linear C_{11} ($D_{\infty h}$, $^1\Sigma_g^+$) predict an extremely intense $\nu_{11}(\sigma_u)$ band at 2126.7 cm^{-1} and a strong but less intense $\nu_{12}(\sigma_u)$ vibration at 1947.2 cm^{-1}. Because this $\nu_{12}(\sigma_u)$ band lies close to the prediction for the $\nu_{12}(e_u)$ band of cyclic C_8 (Table 1), with $^{12}C_{11}$ to $^{13}C_{11}$ and $^{12}C_8$ to $^{13}C_8$ isotopic shifts for the respective modes of -74 cm^{-1} in both cases, the 1817.8 cm^{-1} band would seem to be a candidate for assignment to linear C_{11}. However, linear C_{11} has recently been observed in neon matrices at 1938.6 and 1853.4 cm^{-1} [9]. The assignment of bands appearing in our spectra at 1936.4 and 1849.9 cm^{-1} (Fig. 3) to the $\nu_{11}(\sigma_u)$ and $\nu_{12}(\sigma_u)$ modes of linear C_{11} in argon is consistent with the small red shifts from neon to argon found for all linear carbon clusters that have been identified in both media [9].

There are prominent features appearing in Fig. 1 that are unrelated to cyclic C_8. The band at 1820.8 cm^{-1} has been assigned to the $\nu_5(\sigma_u)$ mode of linear $^{13}C_7$ by Kranze et $al.$ [21], whereas the absorption at 1746.0 cm^{-1}, most evident in Fig. 1(a), remains unidentified. Finally, the weak band at 1803.5 cm^{-1} [Fig. 1(a)] may be assigned to the $\nu_{14}(\sigma_u)$ fundamental of linear C_{13} ($D_{\infty h}$, $^1\Sigma_g^+$) on basis of its proximity to the gas phase value of 1808.96 cm^{-1} [22]. This band correlates with a second band at 1843.9 cm^{-1} (Fig. 3), in agreement with the observations of Krätschmer and Nachtigall [20], which is assigned here as the $\nu_{13}(\sigma_u)$ fundamental of C_{13}. Although both

modes of linear C_{13} give rise to isotopomers that fall within the region encompassed by cyclic C_8 isotopomers, their contribution to the spectrum is negligible because comparatively little C_{13} is formed in our experiments (Fig. 3), which produce predominantly cyclic polycarbons.

Based on FTIR matrix-isolation studies of laser-ablated graphite, Wang et al. [14] recently assigned the 1843.9 cm^{-1} band (appearing at 1844.2 cm^{-1} in their work) to the $\nu_{12}(e_u)$ mode of cyclic C_8. Apparently, they failed to note the correlation between this absorption and the band at 1803.5 cm^{-1}, as seen in our Fig. 3. To better differentiate between those features in the spectrum belonging to cyclic C_8 and those arising from linear C_{13}, we carried out computationally intensive CCSD(T)/cc-pVDZ isotopic shift calculations on cyclic C_8 (Table 1), we performed B3LYP/cc-pVDZ calculations on linear C_{13}, and we altered the experimental procedure to deliberately produce matrices with enhanced yields of large linear polycarbons. The three spectra of Fig. 4, taken from successive annealings of such matrices, show that the intensities of the 1843.9 and 1803.5 cm^{-1} bands grow in concert. Additionally, calculated infrared spectra of unsubstituted and singly substituted isotopomers of linear C_{13} show intensity ratios of the two bands that are consistent with that seen in Figs. 3 and 4. The data presented by Wang et al. [14] show three well defined but unlabeled peaks on the low-frequency shoulder of their 1844.2 cm^{-1} peak, shifted by approximately 0.3, 0.9, and 1.4 cm^{-1}, as well as three labeled peaks at 1837.6, 1830.5, and 1825.3 cm^{-1}. Our analysis suggest instead that all these belong to $^{13}C_1{}^{12}C_{12}$ isotopomers of the $\nu_{14}(\sigma_u)$ mode of linear C_{13}; other bands appearing in their data may be associated with more highly substituted isotopomers. Finally, the band appearing at 1850.9 cm^{-1} in their data, which was assigned to an isotopomer from a previously inactive a_g mode of cyclic $^{12}C_8$, is actually the $\nu_{12}(\sigma_u)$ mode of linear C_{11}, as we have indicated.

Conclusions

Notwithstanding the heavily congested spectra of Fig. 1(b)-(c), we have definitively identified cyclic C_8 through direct comparisons of the measured and calculated isotopic shifts and by identifying other carbon clusters contributing to these spectra. Fourier transform infrared measurements including correlation of isotopomer bands throughout repeated annealings, together with the predictions of *ab initio* calculations, have resulted in assignment of the $\nu_{12}(e_u)$ fundamental at 1817.8 cm^{-1}, correcting an erroneous assignment in the recent literature. Additionally, we have verified assignments of the $\nu_{11}(\sigma_u)$ and $\nu_{12}(\sigma_u)$ fundamentals of linear C_{11}, as well as the $\nu_{13}(\sigma_u)$ and $\nu_{14}(\sigma_u)$ modes of linear C_{13}.

Acknowledgments

References

[1]   See, for example, Proceedings of the High Energy Density Matter (HEDM) Contractors Conference Held 5-7 June 1996 in Boulder CO, eds. P.G. Carrick and N.T. Williams (Phillips Laboratory, Edwards AFB, CA, 1997), U.S. Air Force Report PL-TR-96-3037.

[2]   J.D. Presilla-Márquez, J.A. Sheehy, J.D. Mills, P.G. Carrick, and C.W. Larson, Chem. Phys. Lett. 274 (1997) 439.

[3]   K. Raghavachari and J.S. Binkley, J. Chem. Phys. 87 (1987) 2191.

[4]   J. Hutter, H.P. Lüthi, and F. Diederich, J. Am. Chem. Soc. 116 (1994) 750.

[5] J.M.L. Martin, J. El-Yazal, and J.-P. François, Chem. Phys. Lett. 242 (1995) 570.

[6] J.M.L. Martin and P.R. Taylor, J. Phys. Chem. 100 (1996) 6047.

[7] R.J. Van Zee, R.F. Ferrante, K.J. Zeringue, W.Weltner, Jr., and D.W. Ewing, J. Chem. Phys. 88 (1988) 3465.

[8] J. Szczepanski, S. Ekern, C. Chapo, and M. Vala, Chem. Phys. 211 (1996) 359.

[9] P. Freivogel, M. Grutter, D. Forney, and J.P. Maier, Chem. Phys. Lett. 216 (1997) 401.

[10] C. Liang and H.F. Schaefer III, Chem. Phys Lett. 169 (1990) 150.

[11] D.W. Arnold, S.E. Bradforth, T.N. Kitsopoulos, and D.M. Neumark, J. Chem. Phys. 95 (1991) 8753.

[12] P. Freivogel, J. Fulara, M. Jakobi, D. Forney, and J.P. Maier, J. Chem. Phys. 103 (1995) 54.

[13] K.R. Thompson, R.L. DeKock, and W. Weltner, Jr., J. Am. Chem. Soc. 93 (1971) 4688.

[14] S.L. Wang, C.M.L. Rittby, and W.R.M. Graham, J. Chem. Phys. 107 (1997) 7025.

[15] A.D. Becke, J. Chem. Phys. 98 (1993) 5648.

[16] T.H. Dunning, J. Chem. Phys. 90 (1989) 1007.

[17] Gaussian 94, Revision D.4, M.J. Frisch, G.W. Trucks, H.B. Schlegel, P.M.W. Gill, B.G. Johnson, M.A. Robb, J.R. Cheeseman, T. Keith, G.A. Petersson, J.A. Montgomery, K. Raghavachari, M.A. Al-Laham, V.G. Zakrzewski, J.V. Ortiz, J.B. Foresman, J. Cioslowski, B.B. Stefanov, A. Nanayakkara, M. Challacombe, C.Y. Peng, P.Y. Ayala, W. Chen, M.W. Wong, J.L. Andres, E.S. Replogle, R. Gomperts, R.L. Martin, D.J. Fox, J.S. Binkley, D.J. Defrees, J. Baker, J.P. Stewart, M. Head-Gordon, C. Gonzalez, and J.A. Pople, Gaussian, Inc., Pittsburgh, PA, 1995.

[18] K. Raghavachari, G.W. Trucks, J.A. Pople, M. Head-Gordon, Chem. Phys. Lett. 157

[19] J.D. Presilla-Márquez, C.W. Larson, P.G. Carrick, and C.M.L. Rittby, J. Chem. Phys. 105 (1996) 3398.

[20] W. Krätschmer and K. Nachtigall, in: Polycyclic aromatic hydrocarbons and astrophysics, eds. A. Léger, L. d'Hendecourt, and N.Boccara (Reidel, Dordrecht, 1987), p. 75.

[21] R.H. Kranze, C.M.L. Rittby, and W.R.M. Graham, J. Chem. Phys. 105 (1996) 5313.

[22] T.F. Giesen, A. Van Orden, H.J. Hwang, R.S. Fellers, R.A. Provençal, and R.J. Saykally, Science 265 (1994) 756.

Table 1. Harmonic frequencies (cm^{-1}) of cyclic C_8 at different levels of calculation. Where available, infrared intensities (km/mol) of the active modes are given in parentheses.

Mode	B3LYP/cc-pVDZ	B3LYP/6-311G(2d)	B3LYP/cc-pVTZ	CCSD(T)/cc-pVDZ
$\omega_1(a_g)$	1942	1921	1930	1854
$\omega_2(a_g)$	973	964	969	938
$\omega_3(a_g)$	622	626	623	529
$\omega_4(b_g)$	1905	1904	1907	1837
$\omega_5(b_g)$	1241	1239	1244	1191
$\omega_6(b_g)$	483	485	486	451
$\omega_7(b_g)$	109	120	116	116
$\omega_8(e_g)$	411	423	430	372
$\omega_9(a_u)$	398 (19)	394 (14)	406 (15)	332
$\omega_{10}(b_u)$	348 (~0)	347 (~0)	351 (~0)	316
$\omega_{11}(b_u)$	170 (~0)	195 (~0)	195 (~0)	173
$\omega_{12}(e_u)$	1934 (536)	1928 (557)	1933 (583)	1899
$\omega_{13}(e_u)$	1065 (59)	1058 (67)	1063 (68)	1027
$\omega_{14}(e_u)$	565 (81)	571 (90)	571 (85)	518

Table 2. Observed and calculated (B3LYP/cc-pVDZ) frequencies (cm^{-1}), and their differences, for selected isotopomers of the $\nu_{12}(e_u)$ mode of cyclic C$_8$.
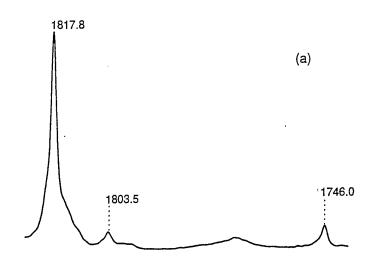
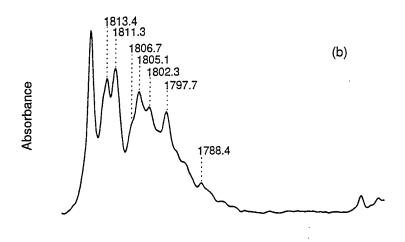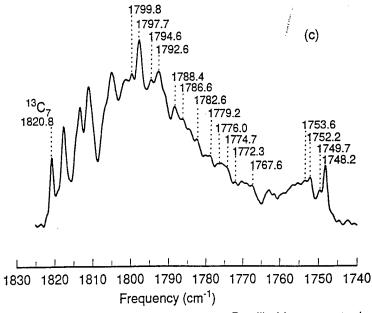| Isotopomer	Stat. Wt.	Observed Frequency		Scaled [a] Calculated Frequency		Difference [b]	
		Mode 12A	Mode 12B	Mode 12A	Mode 12B	Mode 12A	Mode 12B
12-12-12-12-12-12-12-12	1	1817.8	1817.8	1817.8	1817.8	0.0	0.0
13-12-12-12-12-12-12-12	4	1802.3	1817.8	1802.7	1817.8	-0.4	0.0
12-13-12-12-12-12-12-12	4	1805.1	1817.8	1804.6	1817.2	0.5	0.6
13-13-12-12-12-12-12-12	4	1799.8	1817.8	1799.6	1816.8	0.2	1.0
13-12-13-12-12-12-12-12	4	1779.2	1806.7	1778.9	1808.2	0.3	-1.5
13-12-12-13-12-12-12-12	4	1786.6	1811.3	1785.8	1810.6	0.8	0.7
12-13-13-12-12-12-12-12	4	1794.6	1805.1	1793.0	1806.6	1.6	-1.5
13-12-13-12-13-12-12-12	4	1794.6	1806.7	1793.3	1808.7	1.3	-2.0
12-13-13-12-13-12-12-12	2	1776.0	1817.8	1775.3	1817.7	0.7	0.1
13-12-12-13-12-12-12-12	4	1788.4	1813.4	1786.7	1813.2	1.7	0.2
12-13-12-12-13-12-12-12	2	1792.6	1817.8	1791.2	1816.7	1.4	1.1
13-13-13-13-13-12-12-12	4	1748.2	1753.6	1747.3	1751.4	0.9	2.2
13-13-13-13-13-12-13-12	4	1752.2	1767.6	1750.0	1765.9	2.2	1.7
13-13-13-13-12-13-13-12	4	1752.2	1772.3	1749.7	1772.1	2.5	0.2
13-13-13-12-13-13-13-12	2	1749.7	1774.7	1747.5	1774.2	2.2	0.5
13-13-12-13-13-13-13-12	4	1749.7	1774.7	1746.9	1773.1	2.8	1.6
12-13-13-13-13-13-13-12	4	1752.2	1767.6	1749.9	1765.8	2.3	1.8
13-13-13-13-13-12-13-13	4	1752.2	1782.6	1749.6	1780.9	2.6	1.7
13-13-13-12-13-12-13	2	1748.2	1788.4	1746.3	1789.8	1.9	-1.4
13-13-13-13-13-13-13-12	4	1748.2	1752.2	1746.9	1750.9	1.3	1.3
13-13-13-13-13-13-12-13	4	1748.2	1752.2	1746.3	1750.9	1.9	1.3
13-13-13-13-13-13-13-13	1	1748.2	1748.2	1746.3	1746.3	1.9	1.9

[a] The scale factor is 0.939334, as discussed in the text.
[b] These values are the difference between observed and scaled calculated frequencies.

12

Figure Captions

Figure 1. FTIR spectra of the $\nu_{12}(e_u)$ mode of cyclic C_8 measured in matrices annealed to 27.5 K, with average compositions of: (a) natural-abundance carbon; (b) 75% ^{12}C and 25% ^{13}C; and (c) 50% ^{12}C and 50% ^{13}C.

Figure 2. FTIR spectra of matrix (c) after annealing to: (a) 27.5 K for 180 s; (b) 30.0 K for 150 s; (c) 32.5 K for 60 s.

Figure 3. FTIR spectra of the 1650-1955 cm^{-1} region of matrix (a) produced from natural abundance carbon: (a) as deposited; (b) after annealing to 27.5 K for 180 s; (c) after annealing to 30.0 K for 150 s.

Figure 4. FTIR spectra of the 1650-1955 cm^{-1} region of a matrix produced from natural abundance carbon with an enhanced yield of linear C_{13} relative to cyclic polycarbons: (a) as deposited; (b) after annealing to 27.5 K for 180 s; and (c) after annealing to 30.0 K for 150 s.

(a)

1817.8

1803.5

1746.0

(b)

1813.4
1811.3
1806.7
1805.1
1802.3
1797.7

1788.4

Absorbance

(c)

1799.8
1797.7
1794.6
1792.6

1788.4
1786.6
1782.6
1779.2
1776.0
1774.7
1772.3
1767.6

$^{13}C_7$
1820.8

1753.6
1752.2
1749.7
1748.2

1830 1820 1810 1800 1790 1780 1770 1760 1750 1740

Frequency (cm^{-1})

Presilla-Marquez, et al., Fig. 1

Presilla-Marquez, et al., Fig. 2

Frequency (cm⁻¹)

Absorbance

1748.2
1749.7
1752.2
1755.2
1757.0
1759.3
1762.9
1767.6
1769.7
1774.7
1779.2
1782.6
1786.6
1788.4
1792.6
1794.6
1797.7
1799.8
1801.6
1805.1
1811.3
1813.4
1817.8
1820.8

a
b
c

Presilla-Marquez, et. al., Fig. 3

Frequency (cm⁻¹)

Absorbance

Presilla-Marquez, et. al., Fig. 4